EXCHANGES OF KINETIC ENERGY AT THE OCEAN ATMOSPHERE INTERFACE

Привет всем

Part two: A closer look at the Wave-influenced Boundary Layer (WBL) from wind-wave tank data and from a wave-following platform

Thirteenth International Scientific School for Young Scientists
“WAVES AND VORTICES IN COMPLEX MEDIA”

P. Fraunié[*] et D. Bourras

[*]Mediterranean Institute of Oceanography, Université de Toulon, Aix Marseille Université, CNRS 7294, IRD, BP 20832, 83957 La Garde cedex France, fraunie@univ-tln.fr

The LASIF Wind-wave tank of Luminy, Marseille

The LASIF is a 40 m long wind-wave tank built in the early 70's. It is equipped with a programmable wave generation paddle and a controlled fan that blows quasi-laminar air at speeds up to 15 m/s. A wide range of fetches is reachable, from some meters to 30 m. A unique property of the facility is its well-shaped and fully developed turbulent atmospheric boundary layer from the lightest winds (1 m/s). A survey of the available instruments for studying air, wave, and sea properties will be presented, including current sensors, wave gauges, microwave sensors, and PIV and CTA probes. Next, a summary of recent science results obtained at the facility and ongoing activities will be described, they regard both engineering inclined subjects and fundamental wind turbulence-wave studies. The LASIF is fully and easily open to new collaborations, with a specific interest to questions around the reconciliation of open sea data, turbulence theories, and wind-wave tank measurements that account for wind, wave, currents, as well as thermal stratification.

Large Air-Sea Interaction Facility (LASIF) / Grande soufflerie vent-vagues (IOA building)
OSU-Pythéas, IRPHE, MIO, AMU

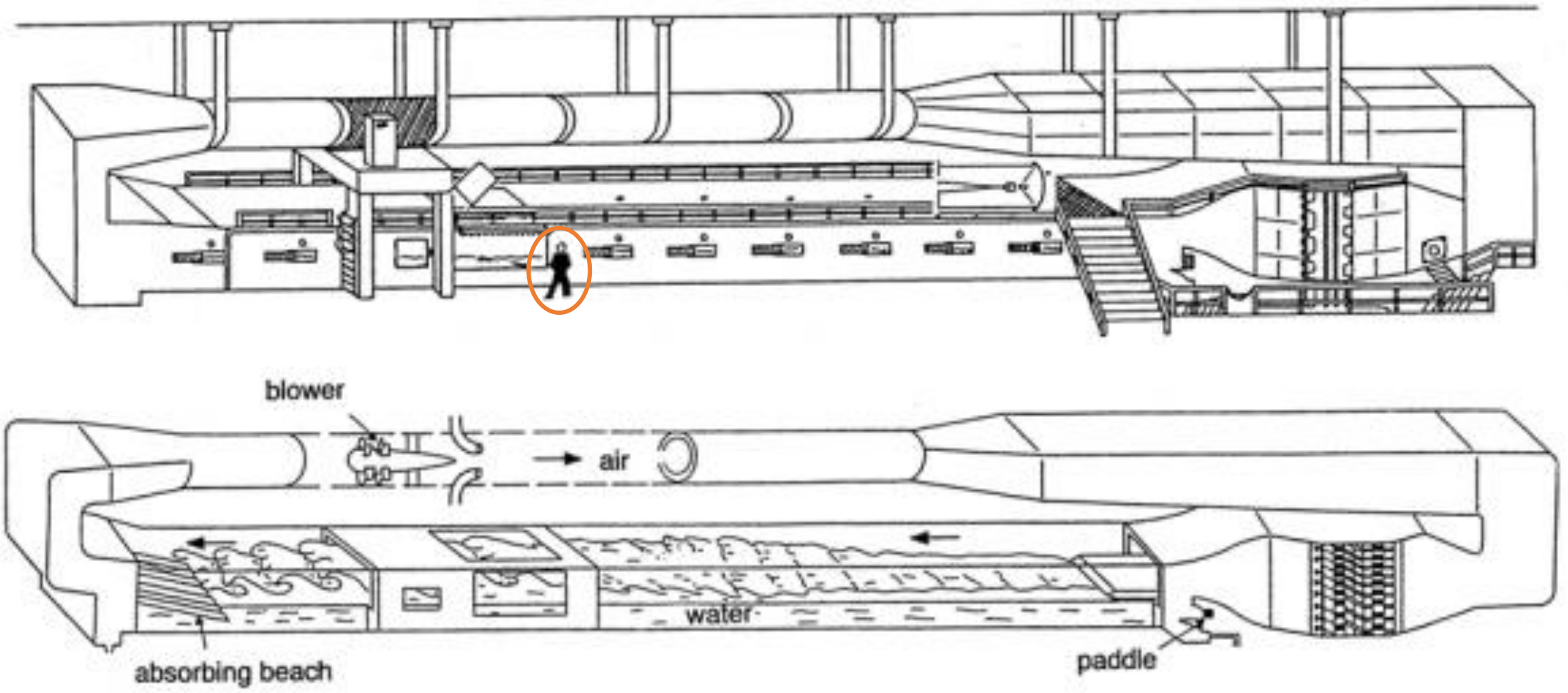

External dimensions : 60 x 3.5m x 7 m

Internal dimensions : 40 x 2.7 x (1.6 m air+0.9 m water)

at low wind speeds (X = 26 m)

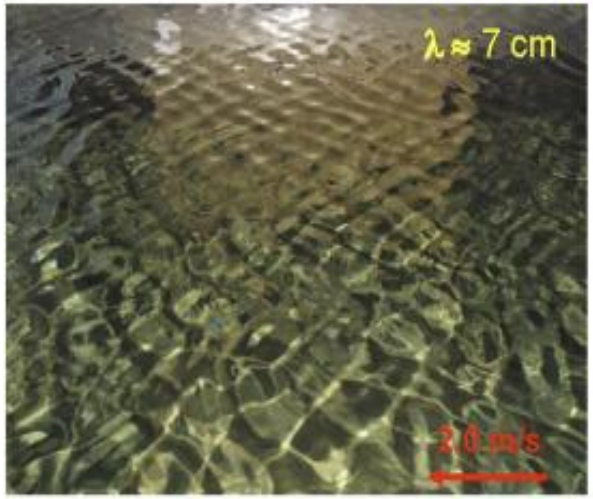

a) Rhombic short wind wave patterns (λ ≈ 7 cm) observed at 2.0 m/s wind speed.

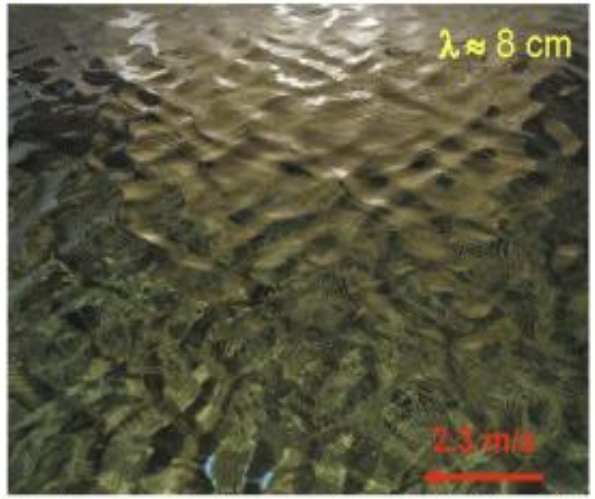

b) Dominant gravity-capillary waves (λ ≈ 8 cm) with intermittent parasitic capillaries at the wavefront observed at 2.3 m/s wind speed.

Example : Wind driven waves

at moderate to strong wind speeds

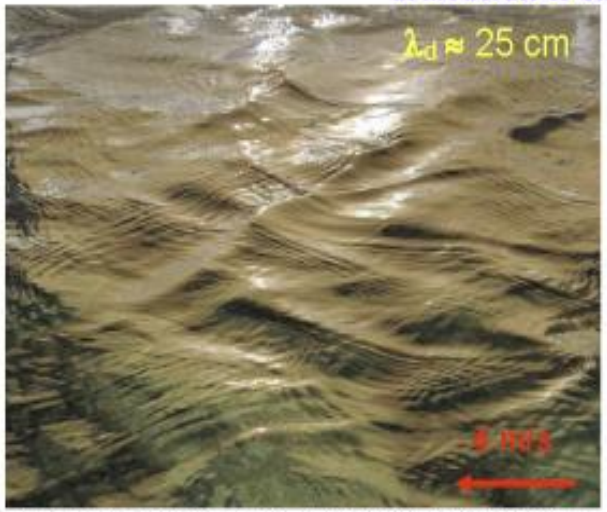

c) Dominant gravity waves (λ ≈ 25 cm) with capillaries at the crest wavefront observed at 4.0 m/s wind speed.

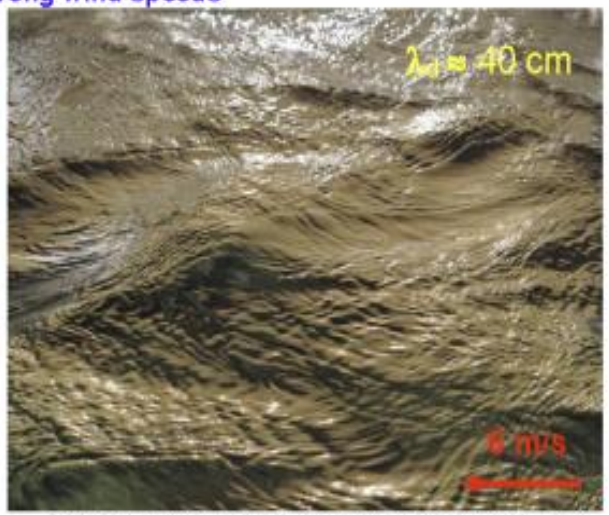

d) Short wind wave roughness generated by wind at the surface of dominant gravity waves (λ ≈ 40 cm) observed at 6.0 m/s wind speed.

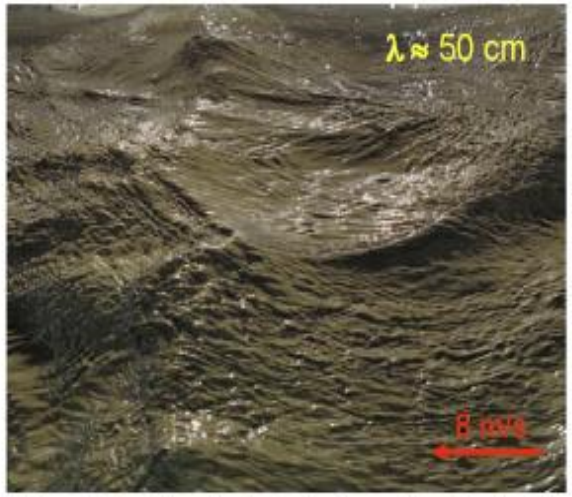

e) Microscale breaking dominant wind waves (λ ≈ 50 cm) with capillaries and wind-generated capillary-gravity waves above as observed at 8 m/s wind speed.

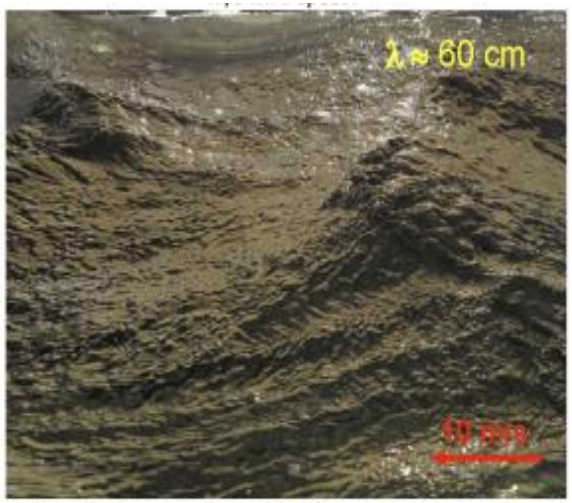

f) Typical crescent-shaped breaking of dominant gravity waves (λ ≈ 60 cm) observed at 10 m/s wind speed.

Fun example : Wave focalization

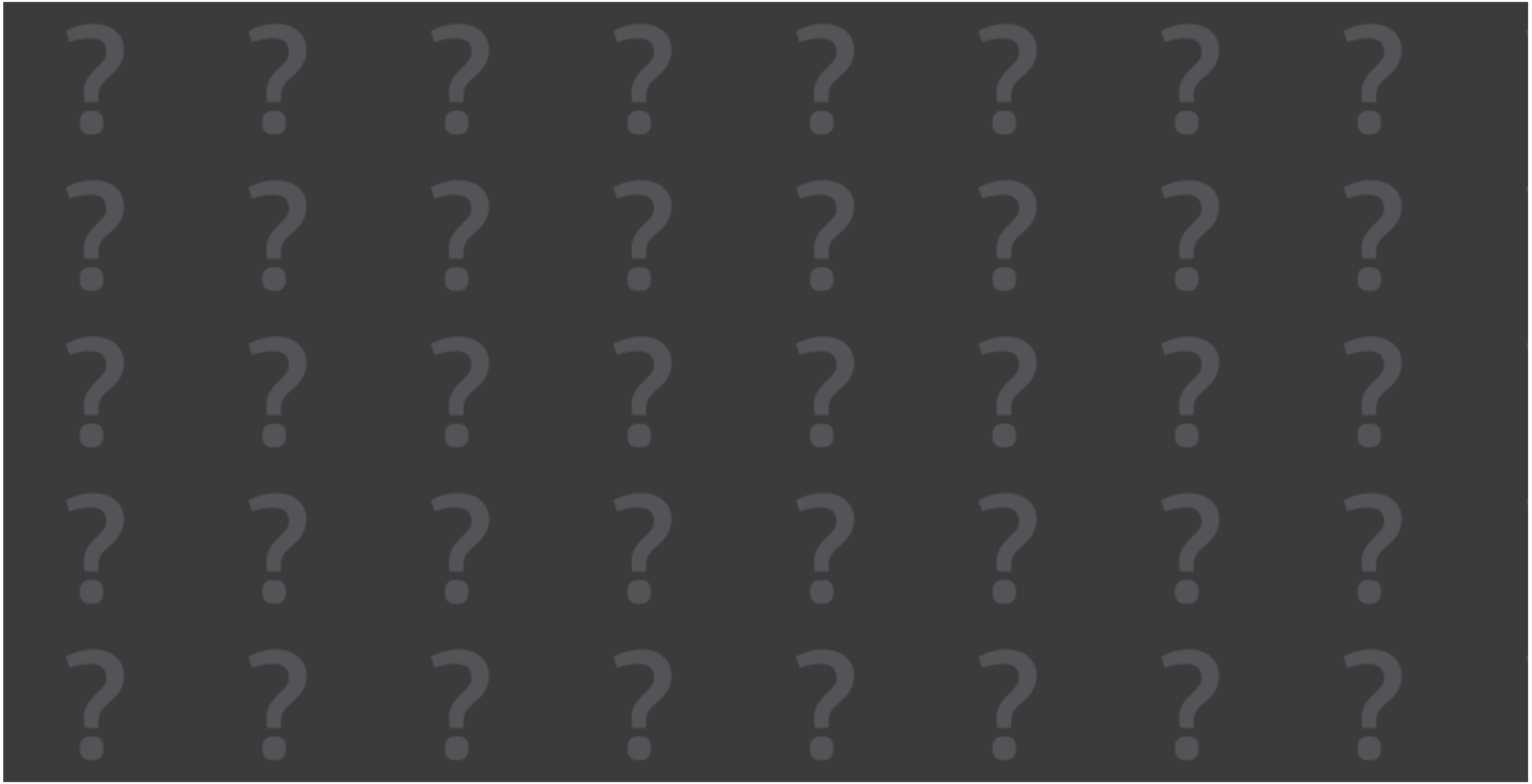

Estimation of the momentum flux over wind-driven waves at the LASIF facility: a revisit

Elpida Vonta, Denis Bourras, Christopher Luneau, and Julien Touboul

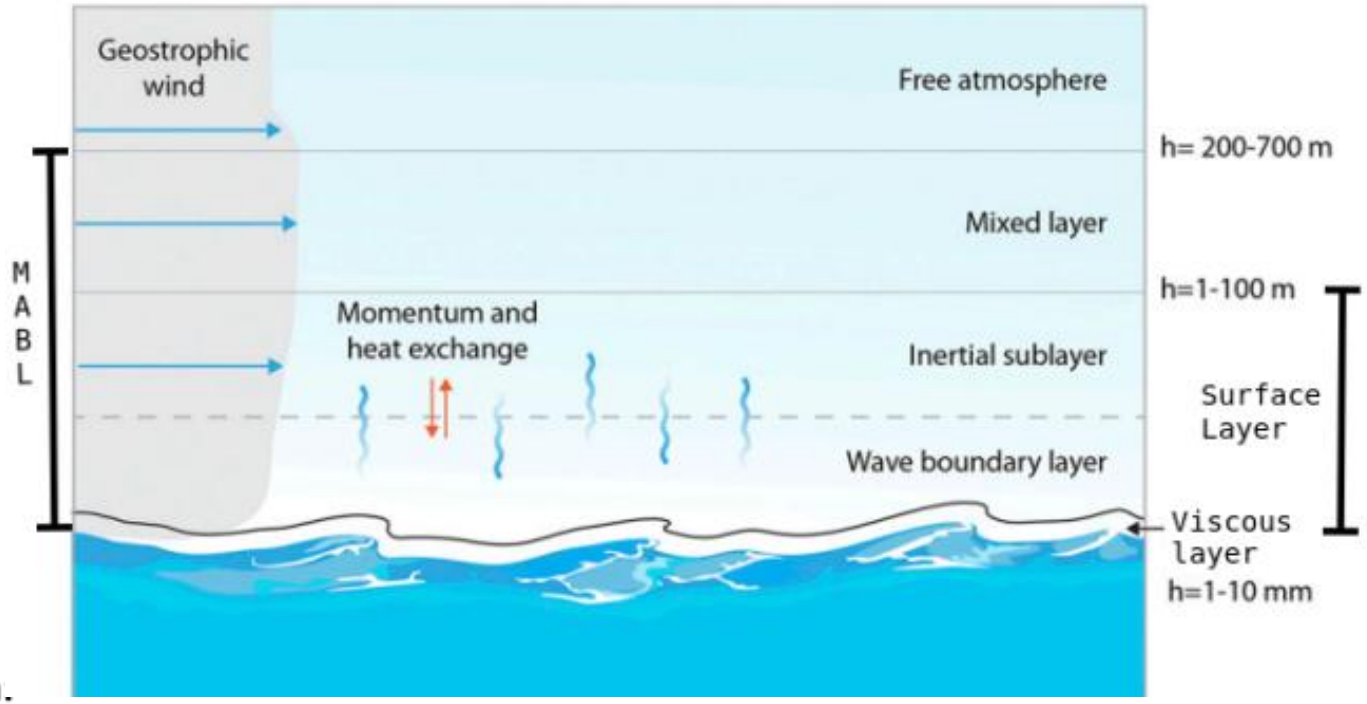

Momentum equation.

$\tau_a(z) = \tau_{turb}(z) + \tau_{waves}(z) + \tau_{visc}(z), where\ \tau_{turb} = -\rho\overline{u'w'} = \rho u_*^2$

Similarity theory: $\tau_a(z) = \rho C_D {U_{10}}^2$

According to the momentum conservation equation, the wind stress above water waves has three components; the shear-induced turbulent stress $\tau_{turb}(z)$ that is responsible for the majority of heat and momentum exchange, the wave-induced stress $\tau_{waves}(z)$ that is significant in the WBL and the viscous stress $\tau_{visc}(z)$ that is important only in the viscous sublayer. This focus of this study was on the inertial or logarithmic part of the BL and as a result only the turbulent component of the wind stress is considered.

Experimental Setup

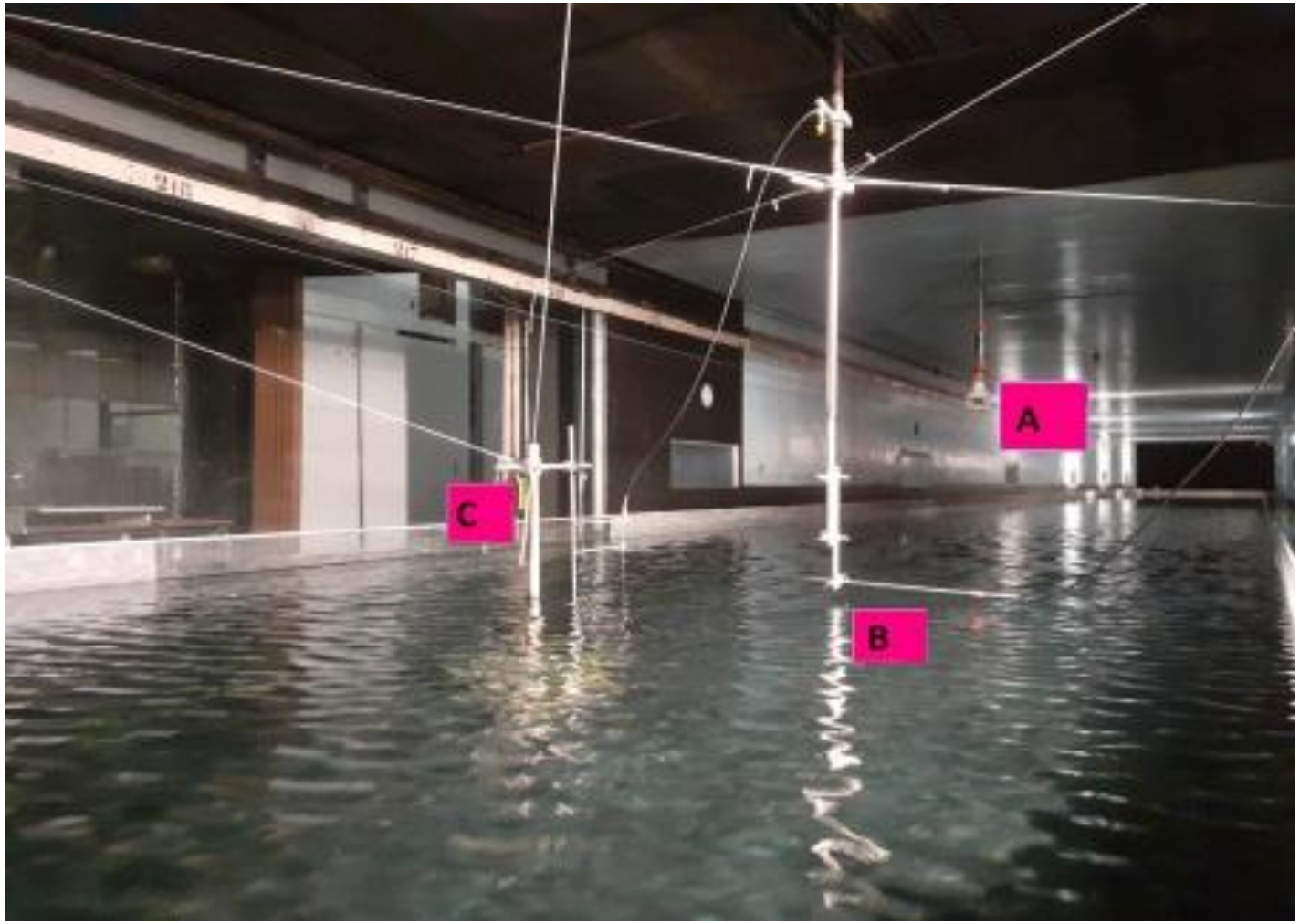

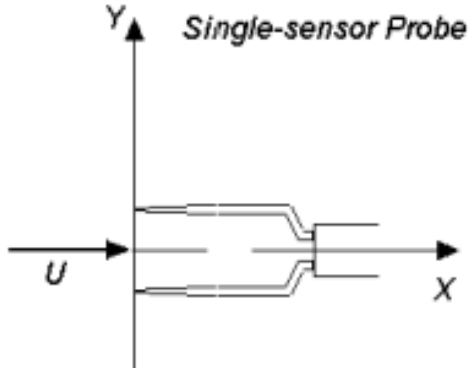

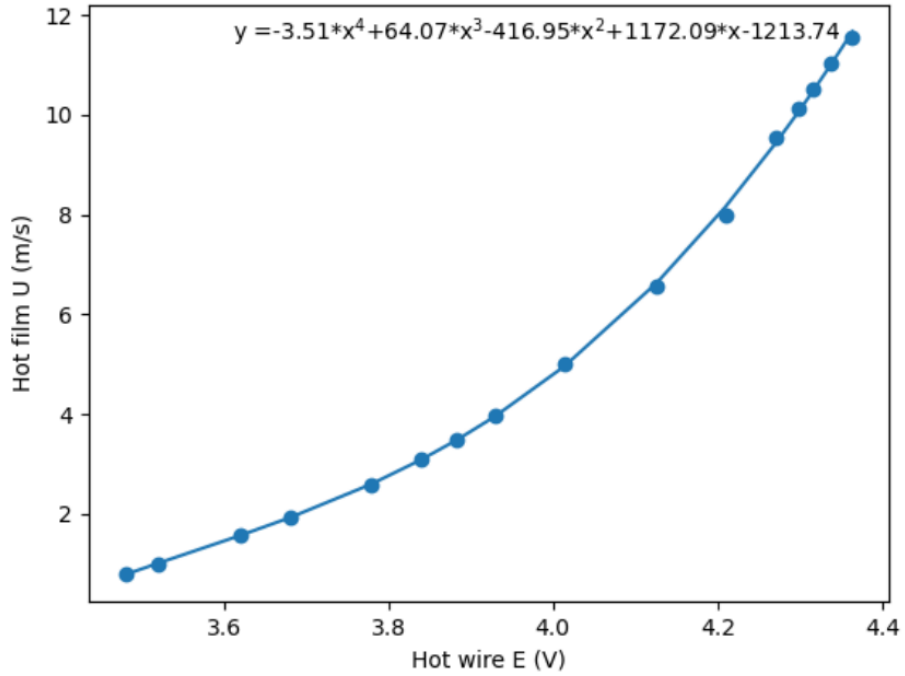

A: Sonic anemometer providing the Uref (m/s) in the middle of tunnel

B: Hot film/Hot wire anemometer providing the U (m/s) close to the water surface

C: Wave gauge providing the wave elevation η (m)

X-wire anemometer

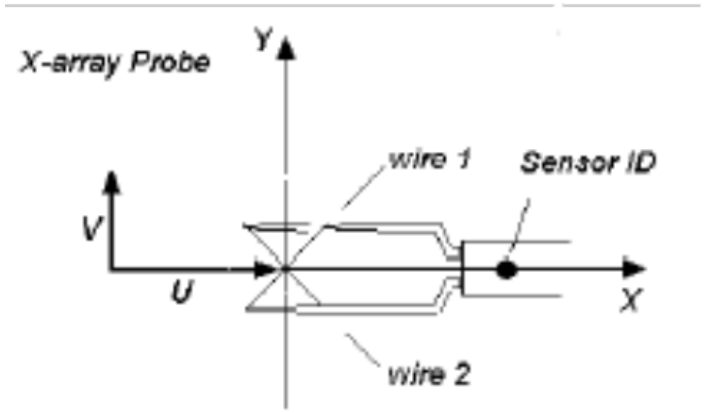

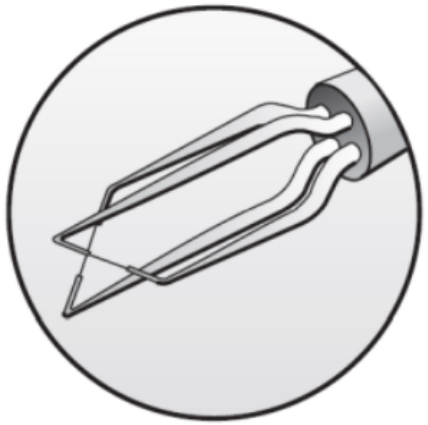

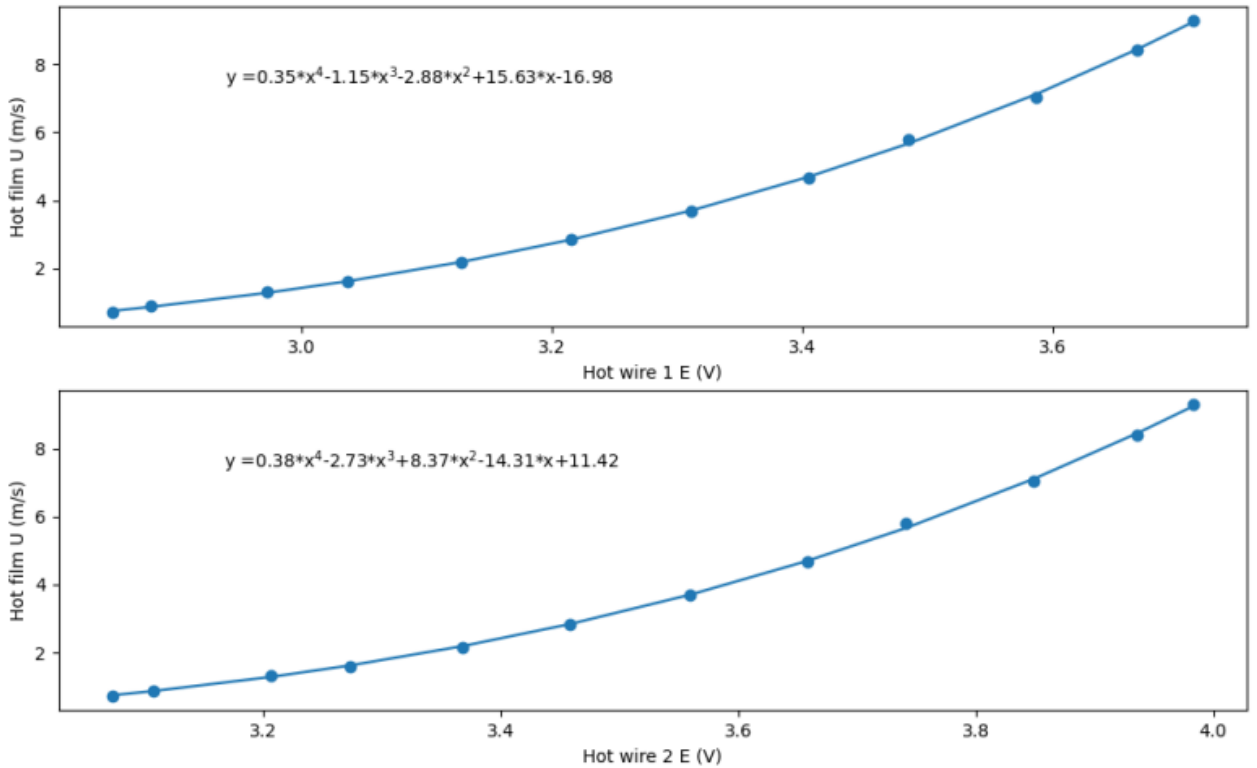

For the X-wire calibration, the sensor was exposed to a range of wind conditions greater than the range of measured wind velocities during the experiment, U=[0.1*$U_{min,exp}$, 1.4*$U_{max,cal}$]= [1, 14] m/s. The sensor was mounted with its prongs parallel to the flow direction, as it appears in Figure 3.6, and the output electric potential E of wires 1 and 2 measured in volts is equated with the output wind velocity U of the hot film measured in m/s in order to obtain one calibration law for every little wire, as it appears in Figure 3.7.

Estimation of the friction velocity u_*

a. Wind profiles method (Hot film sensor):

$$u_* = \frac{1}{\kappa U(z)} log \frac{z}{z_0}$$

b. Inertial Dissipation method (Single hot wire):

$$-\overline{u'w'}\frac{\partial \bar{u}}{\partial z} - \frac{\partial \overline{e'w'}}{\partial z} - \frac{1}{\rho}\frac{\partial \overline{p'w'}}{\partial z} - \epsilon = 0$$

$$u_* = (\kappa z \bar{\varepsilon})^{\frac{1}{3}} \text{ and } \varepsilon = \frac{2\pi}{\bar{u}} f^{\frac{5}{2}} \frac{S_{uu}}{0.55}^{\frac{3}{2}}$$

c. Eddy Covariance method (X wire):

$$\tau = \overline{u'w'} = \rho {u_*}^2$$

Wave measurements

- **Dispersion parameter** $\mu = kd \geq O(1)$

- **Dispersion relation for water waves with surface tension included**

$$\omega^2 = \left(g * k + \frac{\tau_s}{\rho} k^3\right) * \tanh(kd) \text{ , where } \omega = \frac{2\pi}{T_p}$$

Results for the wind profile method

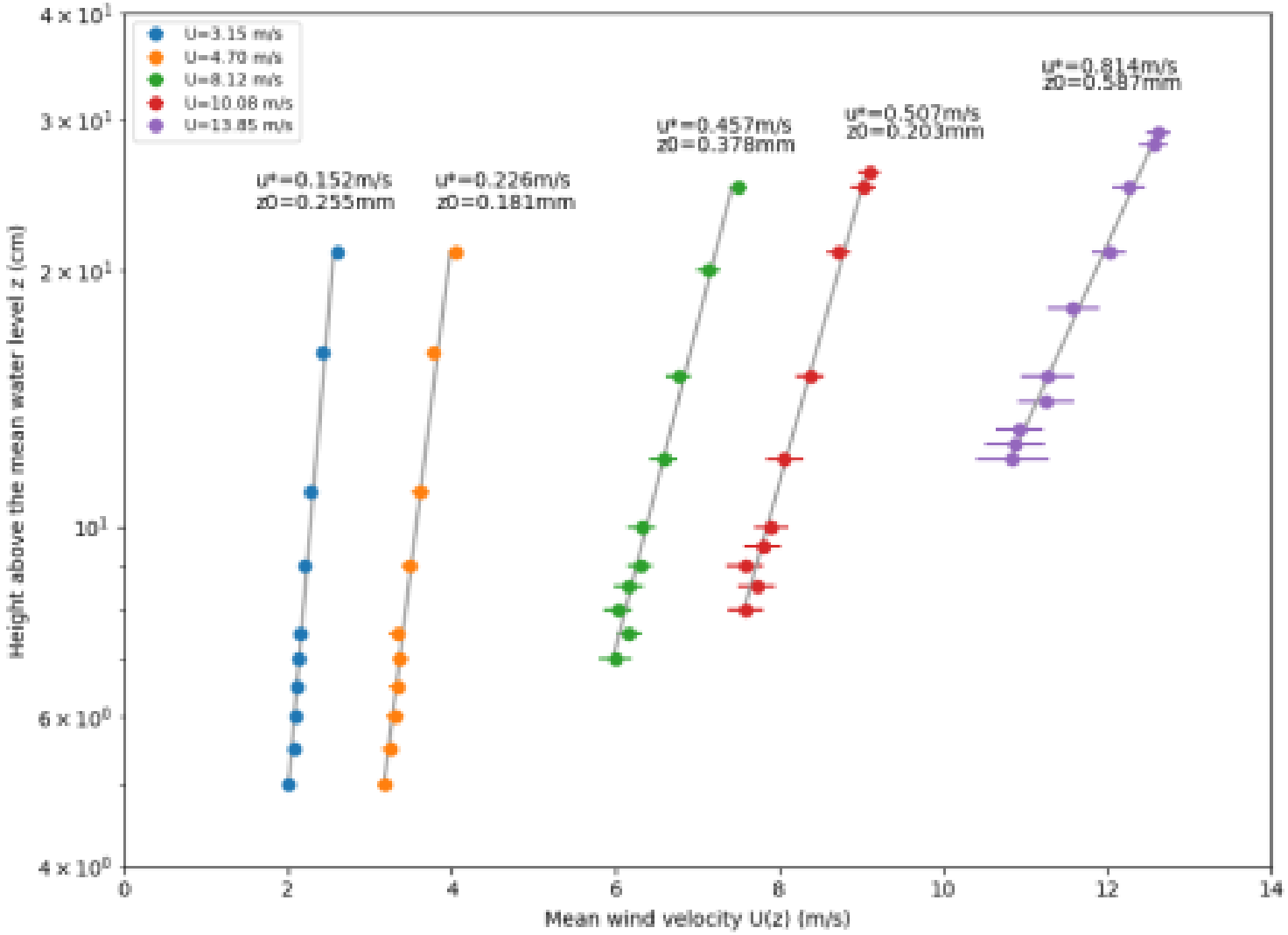

The wind profiles obey the logarithmic law for low wind velocities and this confirms that the measurements are exclusively in the inertia/logarithmic BL. However, for wind velocity greater than 8 m/s the measurements close to the water surface are affected by the waves' presence and it seems that they are in the WBL area. Regarding the u* and the τ_a values, they both increase as the wind velocity increases.

Results for the Inertial Dissipation Method

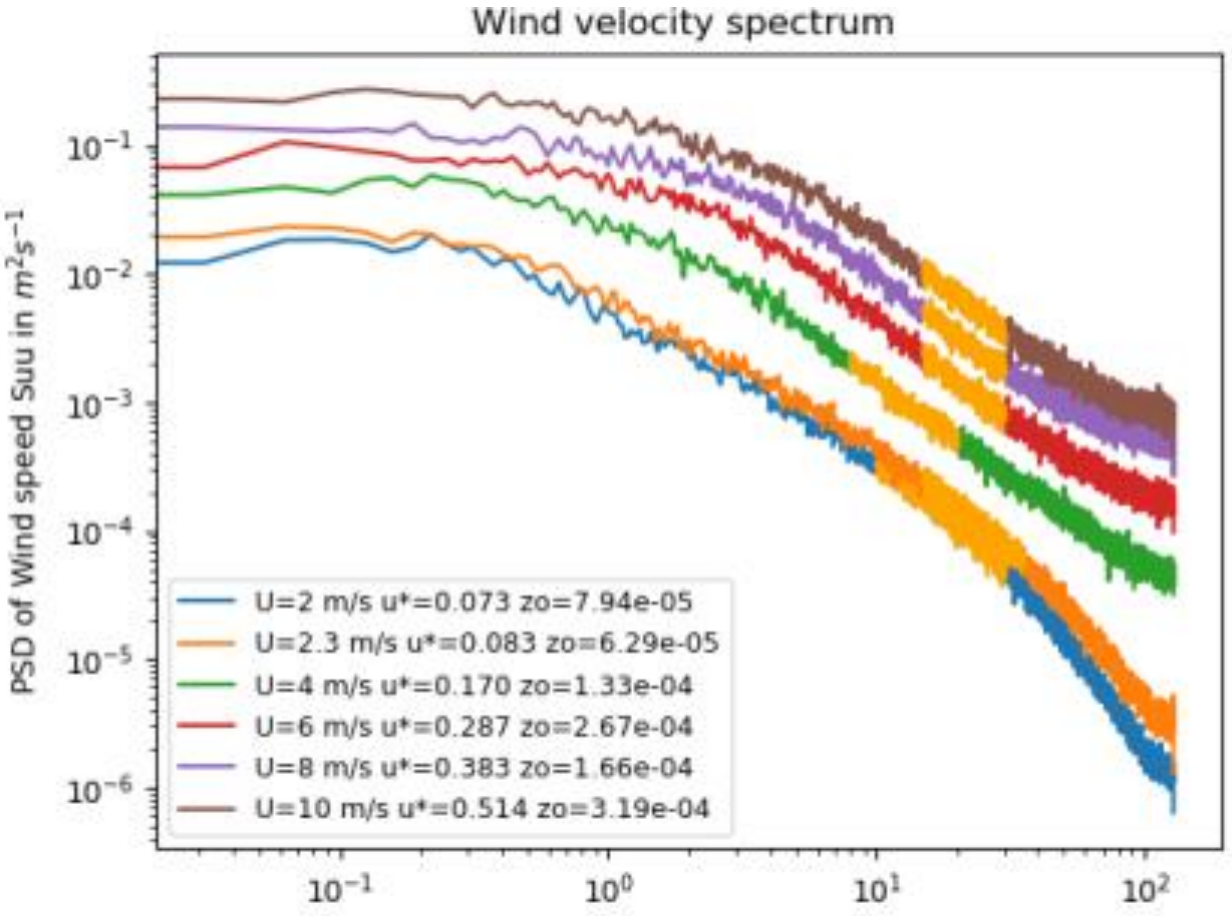

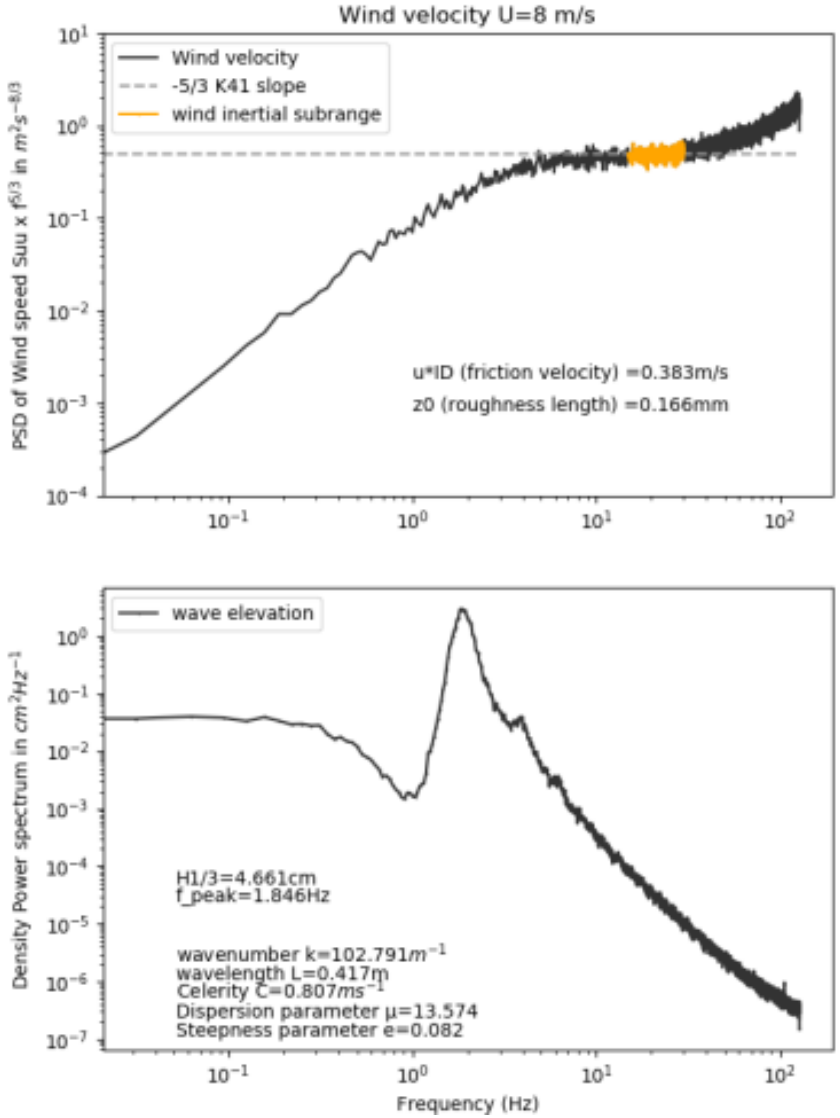

The second experiment was conducted in parallel with the hosted St3ART project that aimed to measure the surface height by an acoustic altimeter and a micro-LIDAR. During this experiment, the wind spectrum was extracted for six different conditions by hot wire measurements. The friction velocity, u*, was estimated throught the ID Method after having calculated the average value of the energy dissipation ε from theinertial zone of the wind spectrum (orange region).

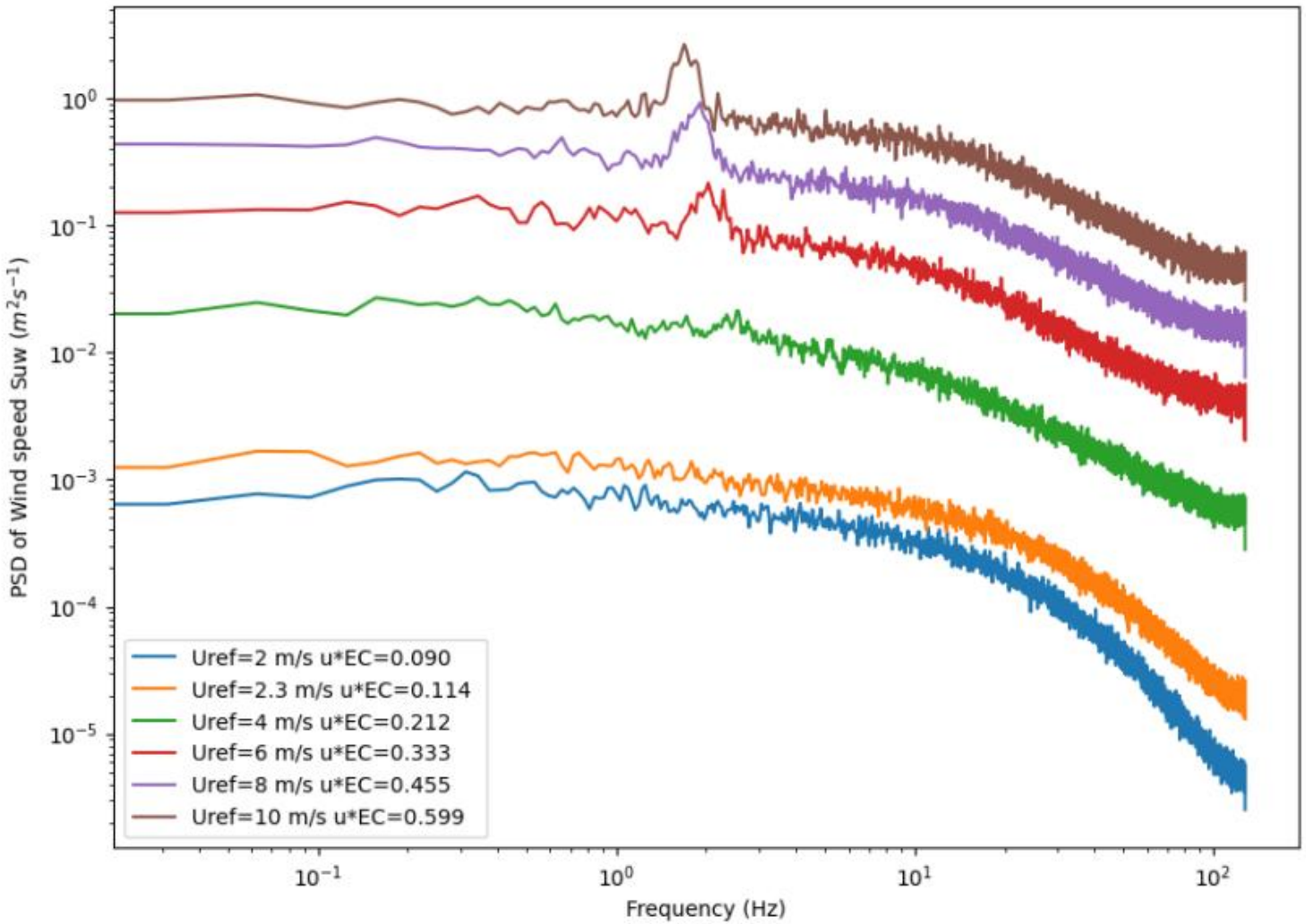
PSD of Wind speed Suw (m^2s^{-1})
10^{0}
10^{-1}
10^{-2}
10^{-3}
10^{-4}
10^{-5}
10^{-1}
10^{0}
10^{1}
10^{2}
Frequency (Hz)
Uref=2 m/s u*EC=0.090
Uref=2.3 m/s u*EC=0.114
Uref=4 m/s u*EC=0.212
Uref=6 m/s u*EC=0.333
Uref=8 m/s u*EC=0.455
Uref=10 m/s u*EC=0.599

What can we learn from recent Large Eddy Simulations (LES)?

Momentum Flux in MABL

As it is mentioned in section 2.3.1, the wind stress over the water surface is not partitioned only to a viscous and a turbulent stress, but there is also a wave-induced component. According to the LES Simulation of Hara and Sullivan (2015), the wave-induced component can be further separated into a wave-fluctuation and a pressure part, as it appears in the Momentum budget of Figure A.1.

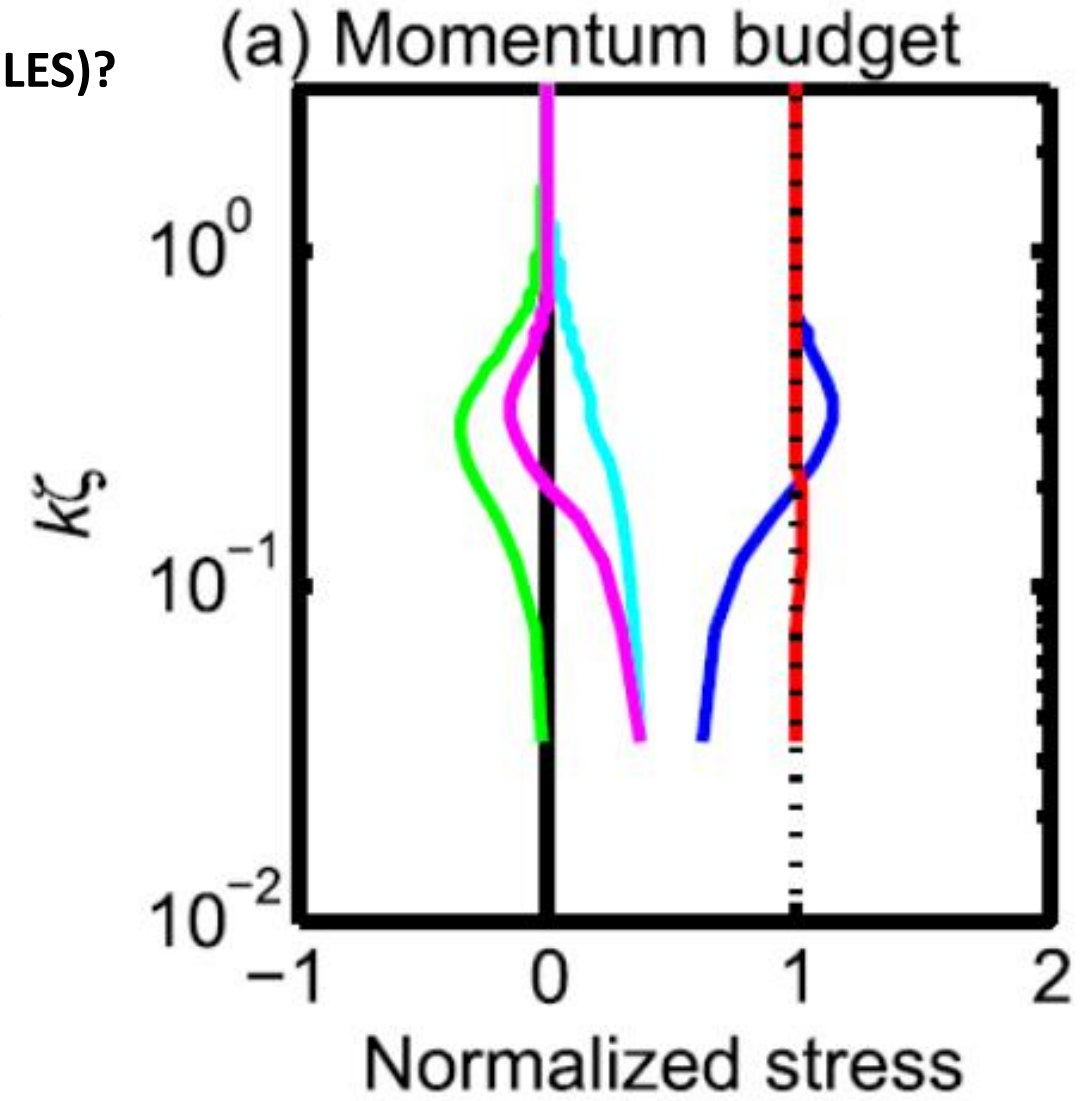

FIGURE A.1: Normalized budget of horizontally averaged momentum flux Hara and Sullivan (2015)

Normalised total stress(red); turbulent stress(blue); Normalised wave-induced stress(magenta); wave fluctuation stress(green); pressure stress(cyan)

According to Bourras et al. (2019), if the imbalance term ϕ_{imb} is applied to the ID Method and the hypothesis of stable conditions in the MABL is considered, the friction velocity corresponding to the total wind stress τ_{total} is given by the following formula.

$$u_{*\mathrm{ID\ imb}} = (\kappa z \epsilon)^{\frac{1}{3}} - \phi_{\mathrm{imb}}{}^{\frac{1}{3}}$$

where $u_*ID = (\kappa z \epsilon)^{\frac{1}{3}}$ and if the friction velocity u_*EC corresponds to the total wind stress τ_{total}, the imbalance term ϕ_{imb} is given by the following relation.

$$\phi_{\mathrm{imb}} = 1 - u_{*\mathrm{EC}}^{-3} \kappa z \epsilon$$

$$\phi_{\mathrm{imb}} = 1 - (u_{*\mathrm{ID}}/u_{*\mathrm{EC}})^3$$

The absolute value of imbalance term ϕ_{imb} calculated here varies between ϕ_{imb}= 0.269 and ϕ_{imb}= 0.657, being in agreement with the the imbalance term ϕ_{imb} of Bourras et al. (2019) that is equal to 0.4 ± 0.15. The imbalance term ϕ_{imb} of Bourras et al. (2019) is measured by the wave-following OCARINA platform in six different experiments in open sea. However, a further laboratory research or an alternative theoretical of the imbalance term would be useful in order to examine why the ϕ_{imb} calculated in Experiment III is negative.

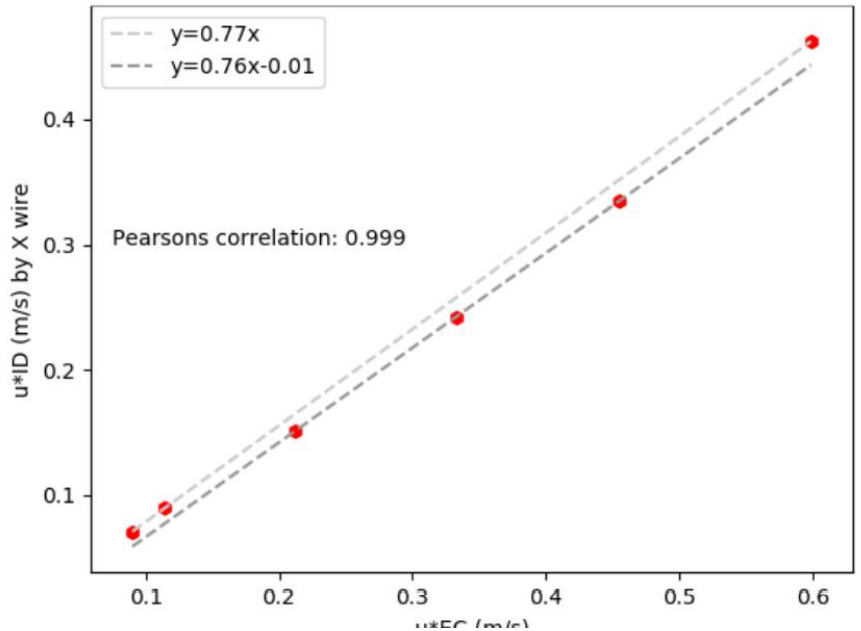

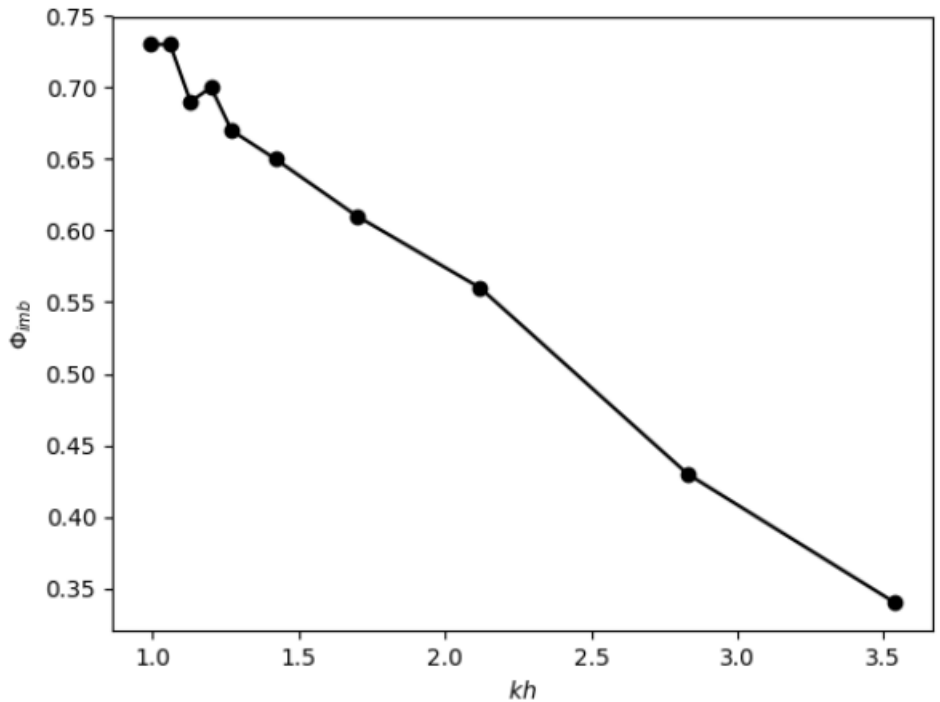

Table 4: *Calculation of the imbalance term ϕ_{imb}, $u_{*_{ID}}$ and $u_{*_{EC}}$ at U_{ref}=8* $\mathrm{m\,s^{-1}}$

kh	$u_{*\mathrm{ID}}$ $(\mathrm{m\,s^{-1}})$	$u_{*\mathrm{EC}}$ $(\mathrm{m\,s^{-1}})$	$u_{*\mathrm{ID}}/u_{*\mathrm{EC}}$	ϕ_{imb}
0.99	0.317	0.491	0.646	0.73
1.06	0.312	0.484	0.645	0.73
1.13	0.236	0.482	0.676	0.69
1.20	0.317	0.476	0.666	0.70
1.27	0.329	0.471	0.689	0.67
1.42	0.327	0.465	0.703	0.65
1.70	0.328	0.451	0.727	0.61
2.12	0.332	0.437	0.760	0.56
2.83	0.340	0.409	0.831	0.43
3.54	0.333	0.383	0.869	0.34

Comparing the friction velocity u_*ID and the friction velocity u_*EC by Experiment III, it is clear that u_*EC is greater than u_*ID for every wind condition. This behaviour can be explained by assuming that u_*ID accounts for the turbulent wind stress $\tau_{turbulent}$ and u_*EC accounts for the total wind stress τ_{total}. Therefore, the u_*EC takes into consideration the momentum flux due to waves' presence and due to viscous effects and the difference between u_*EC and u_*ID could account for the rest of wind stress components apart from the turbulent one; the wave-induced component $\tau_{wave_induced}$ and the viscous component $\tau_{viscous}$.

OCARINA wave-following platform data

$$\phi_{\mathrm{IMB}} = \phi\left(\frac{z}{L}\right) - \frac{z}{L} - \kappa z u_*^{-3} \varepsilon_U$$

The values found for ϕ_{IMB} average to 0.4 ± 0.15.

Before correction

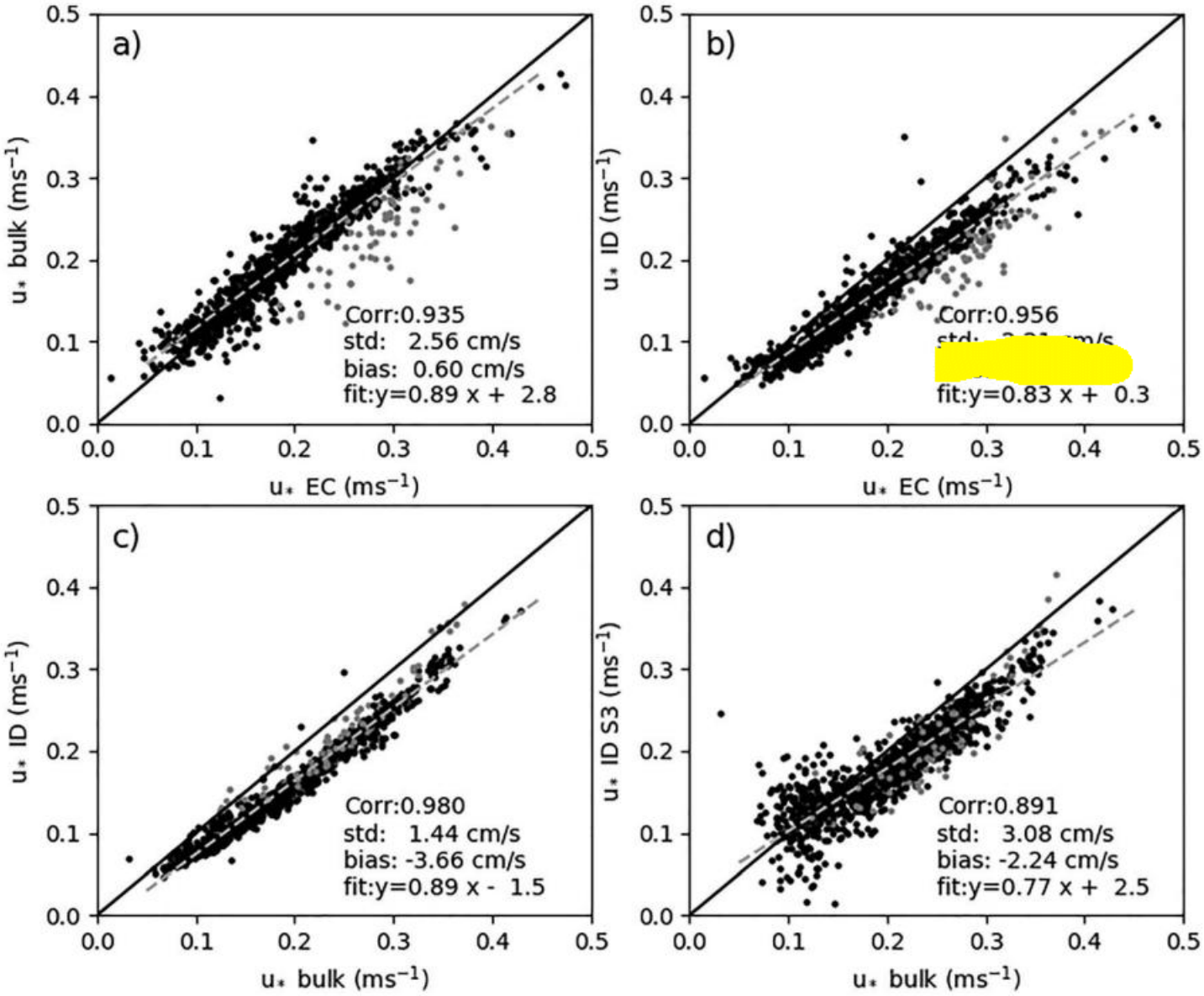

Figure 8. Comparison between friction velocity calculations. Averaged motion correction was applied to EC data. The dots in gray denote B15-2 data. In panel d, the bulk u^* estimates are compared to the ID estimates obtained with third-order structure functions (ID S3; see text).

OCARINA wave-following platform data

After correction (ID and EC)
(Bourras et al. 2019)

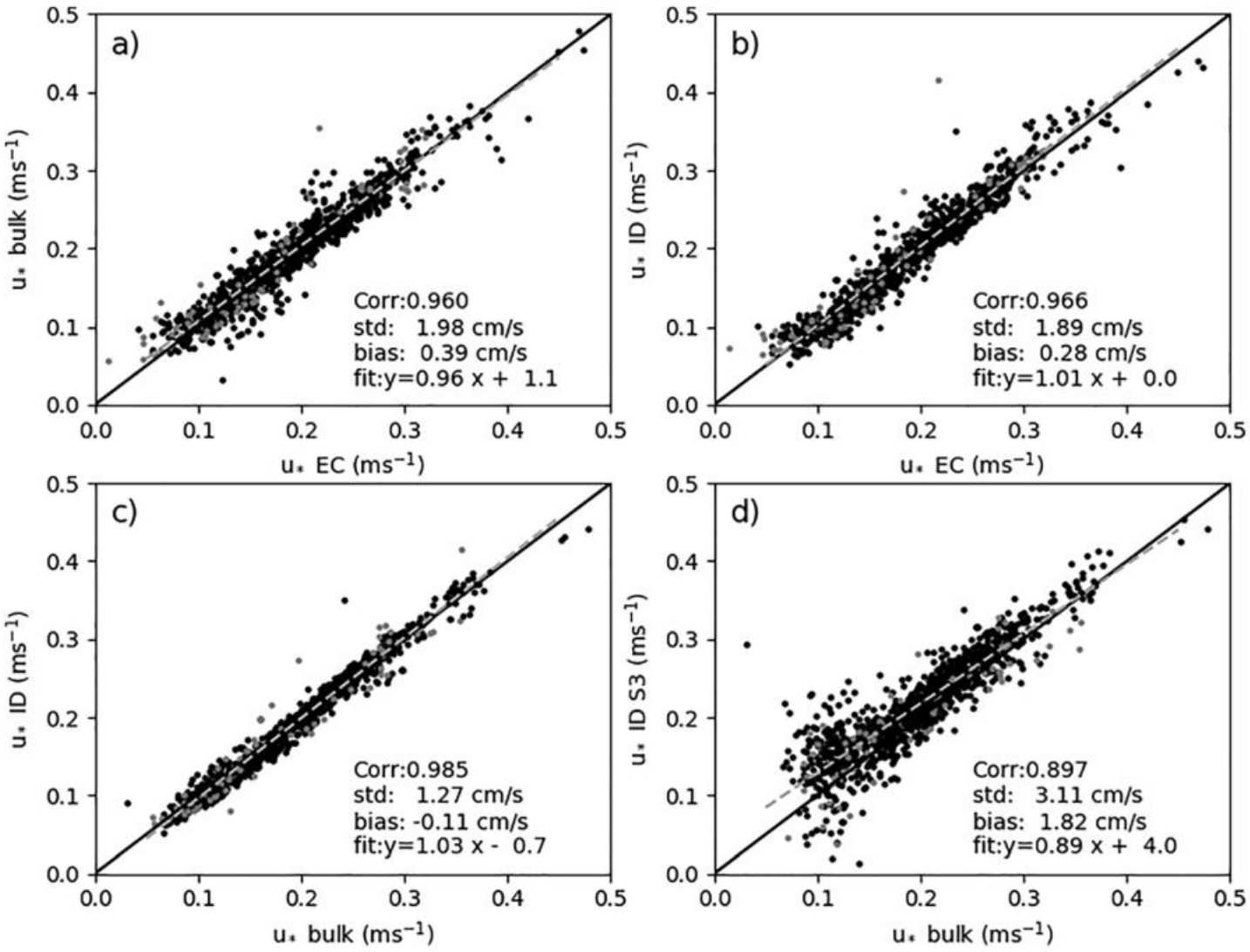

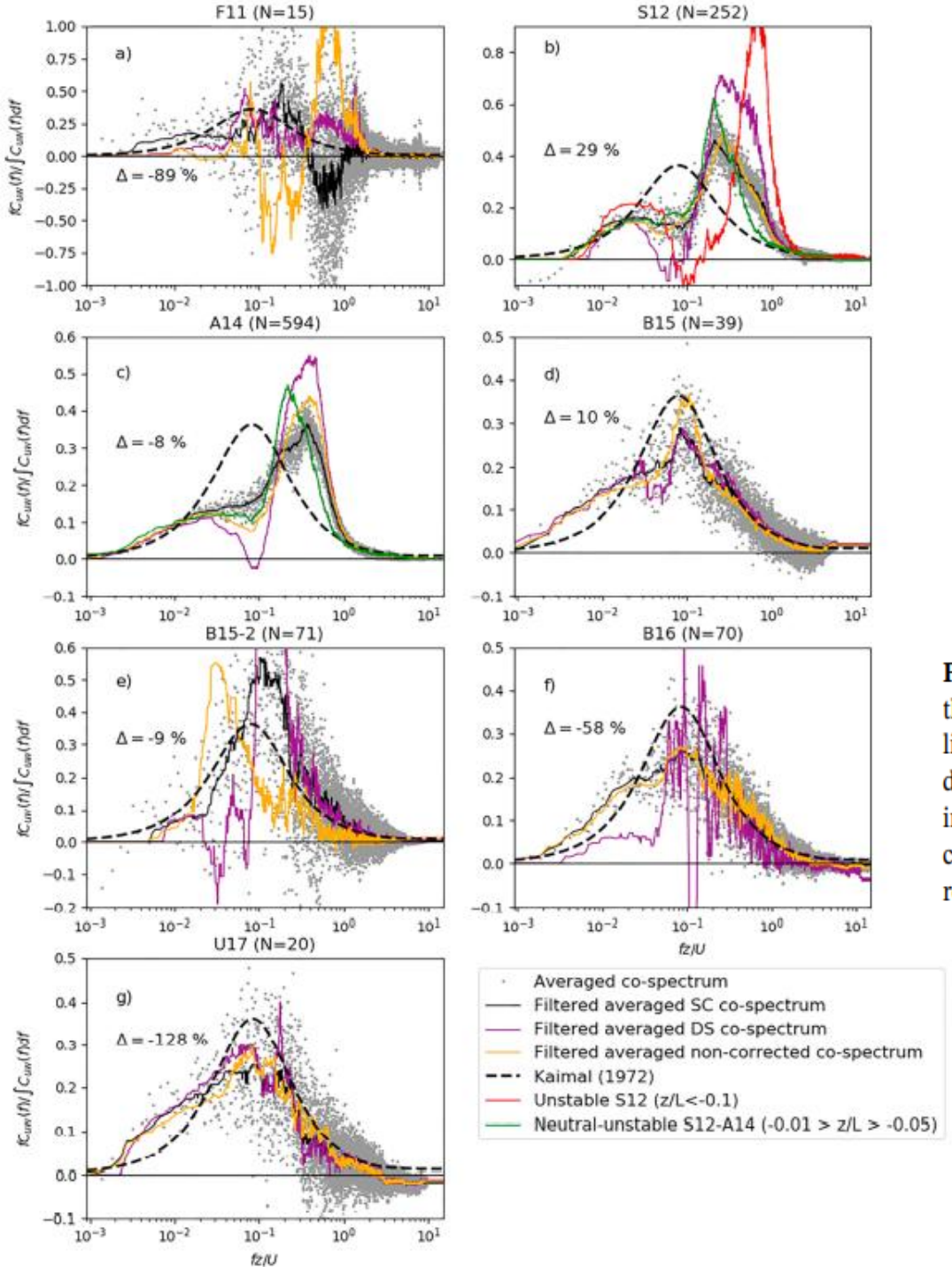

OCARINA wave-following platform data

Should the Kaimal et al. (1972) normalized frequency account for wave characteristics?

Figure 6. Normalized cospectra for the longitudinal wind component (gray dots). The values of *N* in parentheses indicate the number of SC cospectra available for averaging. The dashed curve is the Kaimal et al. (1972) model. The thin black lines correspond to the application of a low-frequency median filter to the gray dots, through all frequencies. The symbol Δ denotes the percentage of difference between the integral values of the averaged SC cospectra with respect to the integral values of the Kaimal et al. (1972) model. Cospectra for the noncorrected and the DS-corrected vertical velocity components are represented in orange and purple, respectively. For S12 and A14 experiments, cospectra are also represented as a function of stability ranges, that is, unstable (red) and neutral-unstable (green).

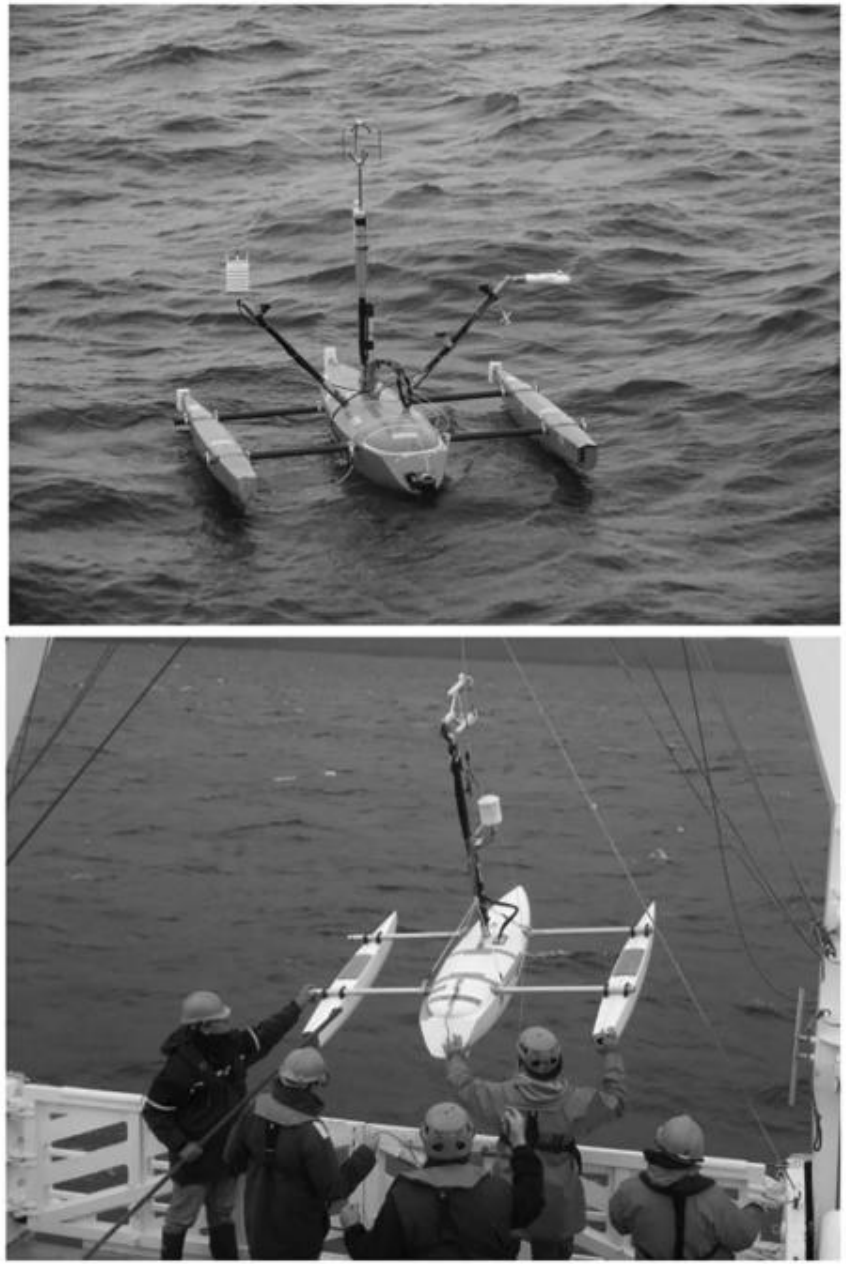

Figure 1. Pictures of the two OCARINA prototypes, referred to as OCARINA #1 (earlier version, upper panel) and OCARINA #2 (more recent test version, lower panel).

OCARINA wave-following platform data

A second puzzling result

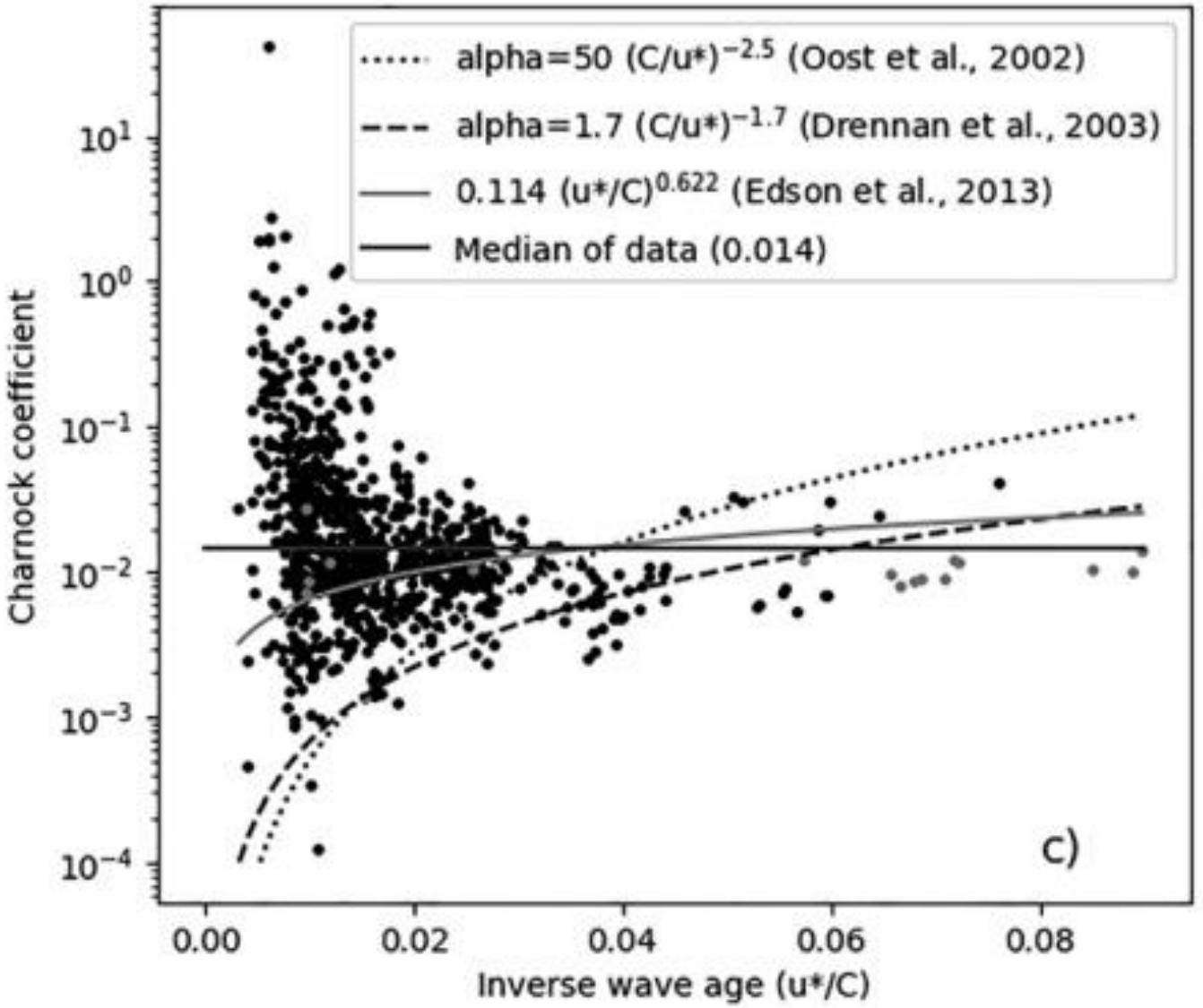

Summary, ongoing and open questions

- Attempt to reconcilate open sea data (OCARINA small ship) with Wind tunnel measurements
  - Phi_imb constant (tau_total vs T_turbulent) ~0.4
  - Open questions
    - OCARINA Cospectra do not fit Kaimal et al. (1972) normalized cospectra (use wave characteristics to normalize frequency?)
    - OCARINA Wave-age do not fit well usual estimates of the Charnock coefficient (for swell, not young waves)
  - Simulations of Hara et Sullivan (2015) gice important clues about what happens close to the waves (in the WBL : Wave Influenced Boundary Layer)
    - Need to better characterize the WBL (for swell, wind-driven waves, mixt regime)
    - Do wind tunnel measurement fit the vertical profile of the vertical momentum flux, component per component (turbulent+wave induced)
  - Heat fluxes : Latent heat flux (LHF) challenging to estimate

Some references

- Large Eddy Simulations
  - T. Hara and P. P. Sullivan, Wave Boundary Layer Turbulence over Surface Waves in a Strongly Forced Condition J. of Physical Oceanography, 45, 868-883, 2015. http://dx.doi.org/10.1175/JPO-D-14-0116.1
- OCARINA wave-following platform: description, code and data
  - Bourras, D. H. Branger, G. Reverdin, L. Marié, R. Cambra, L. Baggio, C. Caudoux, G. Caudal, S. Morisset, N. Geyskens, A. Weill and D. Hauser, A New Platform for the Determination of Air-Sea Fluxes (OCARINA): Overview and First Results J. of Atmospheric and Oceanic Technology, 31, 1043-1062. May 2014. https://doi.org/10.1175/JTECH-D-13-00055.1
  - Bourras, D., R. Cambra, L. Marié, M. Bouin, L. Baggio, H. Branger, H. Beghoura, G. Reverdin, B. Dewitte, A. Paulmier, C. Maes, F. Ardhuin, I. Pairaud, P. Fraunié, C. Luneau, D. Hauser, Air-Sea Turbulent Fluxes From a Wave-Following Platform During Six Experiments at Sea J. of Physical Research: Oceans, 124, 4290-4321. 2019. https://doi.org/10.1029/2018JC014803
  - Bourras, D. R. Cambra, M. Louis, M. Bouin, L. Baggio, H. Branger, H. Beghoura, G. Reverdin, B. Dewitte, A. Paulmier, C. Maes, F. Ardhuin, I. Pairaud, P. Fraunié, C. Luneau, D. Hauser, OCARINA (Ocean coupled to the atmosphere: instrumented research on an auxiliary ship) SEANOE. 2019.https://doi.org/10.17882/59768
  - https://gitlab.osupytheas.fr/bourras.d/albatros_public_distrib
- Recent wind-wave tank results
  - Vonta, L., D. Bourras, J. Touboul, C. Luneau, P. Fraunié, A. Sentchev, A. Villefer, and S. Benjeddou (2022). Imbalance Term in the TKE Budget Over Waves: Preliminary Comparisons Between Open Sea and Wind-Wave Tunnel Measurements, Workshop on Air-Sea Gas Exchanges, 3,4 October, Heidleberg. [submitted]